Solid Phase (REBaO)#Liquid Phase (BaCuO) Reaction: The Way to Highly Oriented ErBaCuO Superconducting Thick Films on Commercial Silver Substrates

M. Muralidhar, N. Sakai, M. Jirsa, and S. Tanaka

Cryst. Growth Des., **2009**, 9 (5), 2404-2408• Publication Date (Web): 11 March 2009

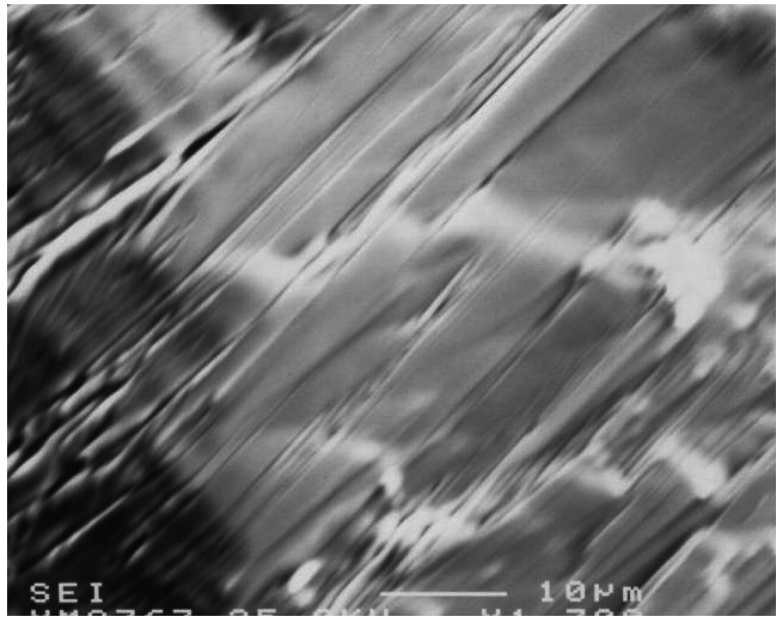

CRYSTAL GROWTH & DESIGN
2009
VOL. 9, NO. 5
2404–2408

Solid Phase (RE_2BaO_4)−Liquid Phase ($BaCuO_2$) Reaction: The Way to Highly Oriented $ErBa_2Cu_3O_y$ Superconducting Thick Films on Commercial Silver Substrates

M. Muralidhar,*,† N. Sakai,† M. Jirsa,‡ and S. Tanaka†

Superconductivity Research Laboratory, International Superconductivity Technology Center, Shinonome 1-10-13, Koto-Ku, Tokyo 135-0062, Japan

Received November 27, 2008; Revised Manuscript Received February 4, 2009

ABSTRACT: Using a solid phase−liquid phase reaction we developed a new technology for preparing *c*-axis oriented thick $ErBa_2Cu_3O_y$ (Er-123) films on commercial polycrystalline silver substrates without the need for a buffer layer. The films were processed in Ar-1% pO_2 atmosphere. Using a double-step annealing, thick Er-123 films were grown, with the onset T_c of about 92 K. Formation of large flat grains with the preferential *c*-axis orientation was confirmed by scanning electron microscopy (SEM), transmission electron microscopy (TEM), and X-ray diffraction. The magnetic self-field critical current density at 77 K was above 40 kA/cm^2. This technology requires only a short processing time and thus is appropriate for utilization in long-length RE-123 silver-sheath wire production.

1. Introduction

In the past two decades, an outstanding endeavor has been carried out after the breakthrough discovery of superconductivity in La−Ba−Cu−O by Bednorz and Muller.[1] The initial transition temperature of about 26 K rose soon above the boiling point of liquid nitrogen (77.3 K) in Y−Ba−Cu−O,[2] which was the most important step toward application of high-T_c superconductors. Large critical current density, J_c, is of a primary importance for development of conductors for high electric power transport. Multifilamentary wires and tapes have been developed in which the superconducting filaments were surrounded by a matrix of a normal metal, such as Cu or Ag, stabilizing the wire/tape against thermal and magnetic flux jumps. Until now three types of superconducting tapes have been developed: polycrystalline BiSCCO tapes (the first generation superconducting wire),[3] YBCO thin-film-based tapes (called coated conductor or second generation superconducting wire),[4] and MgB_2 wires,[5] produced in a similar manner as the BiSCCO ones.

Now the first generation BiSCCO superconducting tapes are in a commercial stage; the high-temperature superconductors (HTSC) industry has produced hundreds of kilometers of the wires for primarily use in power cables and motors. Recently, HTSC coils wound of the BiSCCO tape for a propulsion motor has been designed and tested.[6] Compared to copper wires, the HTSC ones possess nearly the same mechanical characteristics but allow for a much higher current transport due to negligible electric resistivity. Such currents are, of course, associated with rather high magnetic fields created around their paths. And here lies a problem: the irreversibility field (H_{irr}, the field at which vortex lines cease to be pinned and the critical currents fall to zero) at 77 K is in the direction parallel to the *c*-axis only 0.5 T or even less. Although this problem was partly solved by twisting the filaments within the tape, the application of these tapes is limited to rather low magnetic fields and thus also to limited technical currents. Moreover, in comparison with conventional superconducting wires, the applicability of BiSCCO tapes scored only at around liquid helium temperature, 4.2 K, where the difference in operation costs between these two types is negligible.

Scientists also tried to utilize $REBa_2Cu_3O_y$ material (RE = rare earth, RE-123) in a silver tube, similar to the Bibased HTSC wires. In this case, however, the core material (having in principle much better characteristics than BiSCCO) did not exhibit a proper texturing. The main problem was in the fact that the RE-123 crystals grew above the melting temperature of silver and as a result, the grain boundary bounds got weak and the tapes showed poor electromagnetic characteristics.[7]

In the second-generation superconducting ("coated conductor") wires the RE-123 material is utilized in the form of a thin film grown on a flexible metallic substrate covered by a proper buffer layer or layers.[8] It is well-known that the superconductor in the thin film form exhibits the best characteristics, in particular with regard to J_c and H_{irr}. However, for power transport not only critical current *density* is important but much more the total engineering current, I_c. To increase I_c, the tape thickness has to be raised, but with increasing thickness the electromagnetic characteristics rapidly drop. Moreover, growing epitaxial, single-crystalline films in large lengths is very tricky. The films tend to grow polycrystalline and thus the precise alignment and connectivity of grains becomes the basic problem. In thin films biaxial texturing has been shown to help increase grain size and connectivity. However, with increasing film thickness, where also the critical current density rapidly drops, this method loses its power. Thus, up to now, only short lengths of such wires have demonstrated J_c values acceptable for commercial applications, and the maximum thickness, above which the critical current dramatically drops, reached only 1.5 μm.[9] Production of thicker layers by thin film approaches has proved to be ineffective, time-consuming, and costly.

Alternatively, multiple metal−organic depositions (MOD) were tested. Here, compositional gradients and different oxidation levels across the RE-123 film thickness represented a principal disadvantage that led to the overall quality degradation, especially with an increasing number of layers.[10] It was found that the production costs could not be reduced using this process.

* Corresponding author. Present address: Railway Technical Research Institute, Materials Technology Division, 2-8-38 Hikari-cho, Kokubunji-shi, Tokyo 185-8540. E-mail: miryala1@rtri.or.jp.
† Superconductivity Research Laboratory, International Superconductivity Technology Center.
‡ Institute of Physics, ASCR.

10.1021/cg8012987 CCC: $40.75
Published on Web 03/11/2009

We tested a simple and cheap technological process for fabrication of thick RE-123 films that might be useful for commercial applications. Our approach is based on recently conducted experiments on growing $REBa_2Cu_3O_y$ (RE-123) in a microgravity environment in the unmanned space experiment recovery system (USERS), where a solid phase RE_2BaO_4 (RE-210)−liquid phase $BaCuO_2$ reaction was explored.[11] Quench experiments conducted on RE-210 and $BaCuO_2$ showed that a product with a dominant RE-123 phase could be obtained below the melting temperature of silver.[12]

In this paper we report on the first successful deposition of well *c*-axis oriented Er-123 thick superconducting films on commercial polycrystalline silver substrates and their properties.

2. Experimental Methods

High purity commercial powders of Er_2BaO_4, $BaCuO_2$, and CuO were mixed in a nominal composition of $ErBa_2Cu_3O_y$ and Er-rich $Er_{1.2}Ba_2Cu_3O_y$. The powders were ball milled for 4 h, in order to reduce particle size to <100 nm. Then they were air-dried in air, vaccuum-dried at 650 °C for 6 h, and finally cooled to room temperature. By a thorough grinding of the 100 nm sized powder mixed with a wetting agent of α-terpineol and 2-ethyl acetate a highly dense paste was prepared. The paste was spread on a MgO single crystal (later on a commercial silver tape 0.2 mm thick) by means of a well-known screen-printing technique using a 165-mesh screen. The thermal stability of these samples was analyzed by differential thermal analysis (DTA) in Ar-1% pO_2 atmosphere. DTA experiments were carried out in Pt cups by means of the MAC SCIENCE TG-DTA 2000S setup, with a gas flow rate of 50 mL/min and a heating rate of 5 °C/min. The phase transition temperature was determined as the onset temperature in the DTA peak in the final heating process. For the film growth, the covered substrate was placed into a tube furnace and heated up to a maximum temperature lying between 900 and 990 °C at a rate of 200 °C/h. The film was held for 3 h at this temperature and then cooled to room temperature at a rate 50 °C/h. The holding temperature and the starting particle size appeared to be most important factors to produce highly oriented thick films. The crystallographic structure of the films, with special respect to the Er_2BaO_4, $BaCuO_2$, CuO, and Er-123 content ratio, was determined by means of the high-resolution automated X-ray powder diffractometer RINT2200. For magnetic measurements small specimens with dimensions of $a \times b \times c = 1.5 \times 1.5 \times 0.5$ mm^3 were cut from the as-grown films and annealed in flowing O_2 gas in the temperature range 600−450 °C for 36 h. The microstructure of these samples was studied with scanning electron microscopy (SEM) and transmission electron microscopy (TEM). Magnetization hysteresis loops ($M-H$ loops) in fields from −2 to +3 T were measured at 77 K using a commercial SQUID magnetometer (Quantum Design, model MPMS7). To minimize field inhomogeneity, the scan length of the sample holder was set to 10 mm. The external magnetic field was applied parallel to the *c*-axis of the sample. The magnetic J_c values were estimated based on the extended Bean critical state model using the relation

$$J_c = 2\Delta m/[a^2 d(b - a/3)]$$

where d is the sample thickness, a, b are cross-sectional dimensions, $b \geq a$, and Δm is the difference of magnetic moments during increasing and decreasing field in the $M-H$ loop.[13]

3. Results and Discussion

Figure 1 presents schematically the differential thermal analysis (DTA) curves of the conventional route (reaction 1, Figure 1a) and of the solid phase−liquid phase reaction (reaction 2, Figure 1b). In both these routes the final product is the RE-123 phase. The main difference is in utilization of RE-210 in process (2). This results in growth of large plate-like RE-123 crystals at a significantly lower temperature than in the conventional process (1), due to melting of the liquid phase well below the melting temperature of RE-123 (Figure 1).

conventional process: 2 RE-123(→RE-211 + $3BaCuO_2$ + 2CuO) → 2RE-123 (1)

new process: RE-210 + $3BaCuO_2$ + 3CuO → 2 RE-123 (2)

In the experiment in Figure 1a, a downward (endothermic) peak P′ appears at high temperatures. The dip indicates that the RE-123 powder dissolves and absorbs heat. This temperature rises with increasing RE ion radius but is usually at around 1000 °C.

In Figure 1b two endothermic peaks P_1 and P_2 are seen. Confronting these peaks with X-ray diffraction data of the samples rapidly cooled (quenched) from high temperatures, we learned that at the endothermic P_1 peak $Ba_xCu_yO_z$ started to melt at the beginning of the peak so that a liquid phase (probably close to $BaCu_2O_3$, see reaction 2) formed, wetted the solid phase (RE-210), and reacted with it. This enabled formation of the RE-123 phase at temperatures already slightly above P_1. This

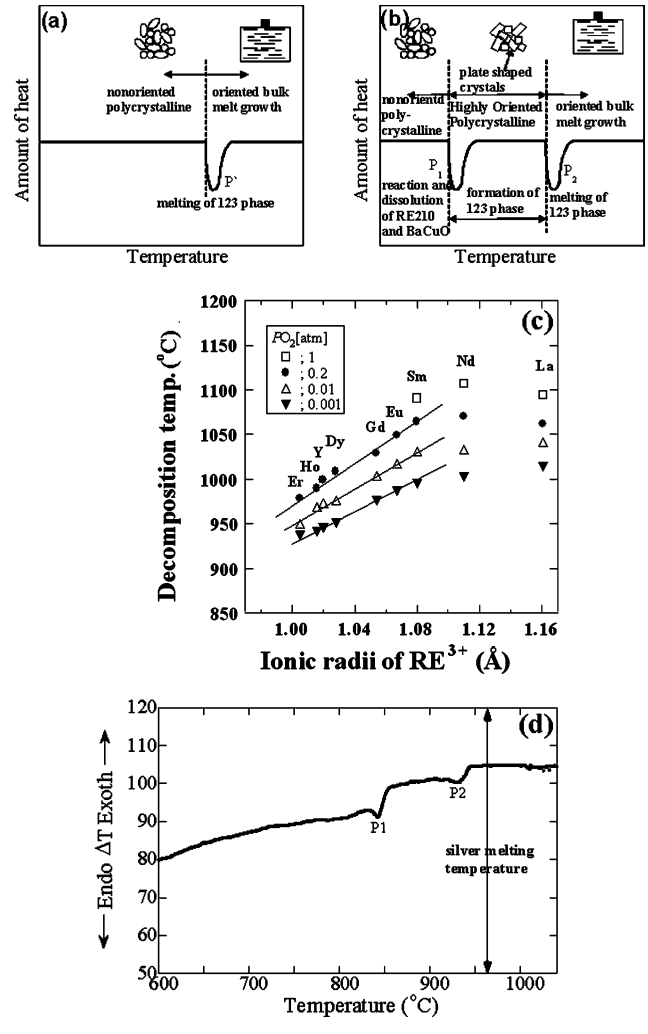

Figure 1. (a) A schematic differential thermal analysis (DTA) curve for the case of heating $REBa_2Cu_3O_y$ powder in the conventional method (reaction 1). (b) A schematic DTA curve for heating a mixture of RE_2BaO_4 and $Ba_xCu_yO_z$ (reaction 2). (c) The peritectic decomposition temperature of RE-123 for various oxygen partial pressures as a function of RE ionic radius. (d) The experimentally observed DTA curve of the mixed powder (100 nm) of Er_2BaO_4, $BaCuO_2$, and CuO.

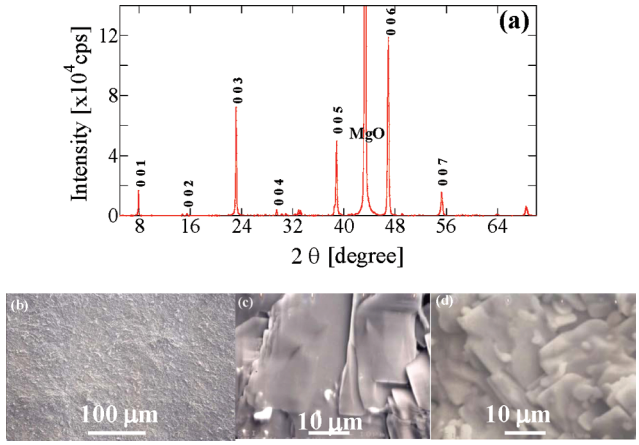

Figure 2. X-ray diffraction (XRD) patterns for $ErBa_2Cu_3O_y$ thick film, prepared on MgO substrates from the mixture of Er_2BaO_4, $BaCuO_2$, and CuO. The films were processed at 950 °C in Ar-1% pO_2 atmosphere (a). High- and low-magnification SEM micrographs of $ErBa_2Cu_3O_y$ thick films on MgO substrate (b−d). Note the relatively large flat and dense surface grains morphology.

process was interrupted and the RE-123 phase melted at temperatures above the P_2 minimum (hereinafter referred to as the P_2 temperature). A polycrystalline structure consisting of large grains formed between temperatures P_1 and P_2, and we found the product to be RE-123 phase with a uniform *c*-axis crystallite orientation.

At temperatures lower than P_1, an arbitrarily oriented RE-123 oxide grew by a solid phase−solid phase reaction. On the other hand, at temperatures above P_2, the RE-123 phase melted. (The conventional melt growth of the RE-123 phase could be used in the temperature range above P_2, using a seed crystal and supercooling.) For our approach it is substantial to ensure that both temperatures, P_1 and P_2, lie reasonably below the melting point of Ag, 960 °C. The broader the (P_1, P_2) temperature interval, the better conditions are for creation of good quality superconducting films. Our extensive study of the effects affecting the P_1 and P_2 temperatures identified the following important factors: (i) reduction of the grain size of the input mixed material to less than 100 nm using a ball milling process; (ii) lowering the oxygen partial pressure in the reaction atmosphere; (iii) adding a small amount of silver to the input powders; (iv) optimization of the $Ba_xCu_yO_z$ compound composition.

In Figure 1c, the peritectic decomposition temperature of RE-123 (the upper temperature limit P_2) as a function of the ionic radius of RE for three different oxygen partial pressures is shown. It is evident that the P_2 temperature decreases with decreasing RE^{+3} ion radius and with decreasing oxygen partial pressure. The lowest decomposition temperature of the whole RE family belongs to Er-123 and at low oxygen partial pressures the P_2 temperature of Er-123 lies well below the melting point of silver. We therefore selected Er-123 as the best choice for further tests for fabrication of thick superconducting films. It also follows from the figure that a low oxygen partial pressure is substantial for keeping the P_2 temperature low. We chose 1% pO_2 as an optimum. Here we note that according to Figure 1c, though not ideal, also Ho, Y, and Dy are appropriate for exploring the new technology for fabrication of RE-123 films. Especially Y might be attractive for its extensive use in previous research.

In the first stage we prepared Er-123 films on MgO substrates. Figure 2a shows typical X-ray diffraction patterns of the

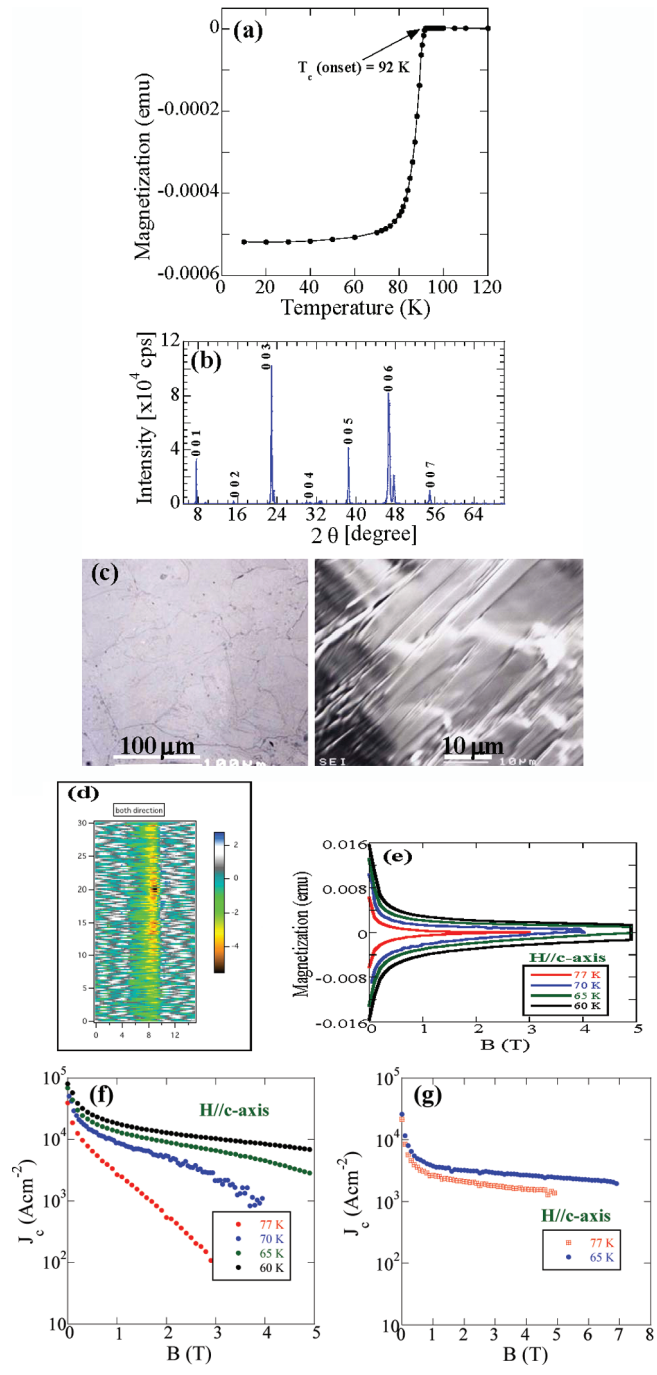

Figure 3. (a) Temperature dependence of DC magnetic moment and (b) the XRD pattern of the $Er_{1.2}Ba_2Cu_3O_y$ film around 10 μm thick on Ag substrate prepared in the double-step process. (c) Scanning electron micrograph (SEM) of the top surface shows formation of a plate-like crystalline microstructure, similar to that of the BiSCCO system. (d) The contour map of stray field distribution obtained by scanning Hall probe (screening currents) indicates the film is quite homogeneous. (e) Magnetization hysteresis loops at and below 77 K and (f) the associated critical current density, J_c, as a function of magnetic field. (g) J_c of the of the $Er_{1.2}Ba_2Cu_3O_y$ sample with a small quantity of Gd-123 added. In this case a significant increase of irreversibility field was observed.

$ErBa_2Cu_3O_y$ films grown on MgO single-crystalline substrate at 950 °C in Ar-1% pO_2 atmosphere. The prominent peaks were identified as (0,0,l) reflections of the Er-123 phase. This indicated that the *c*-axis of the film was well aligned along the substrate normal. Figure 2b shows the film surface in low-magnification SEM. The low-magnification image shows a

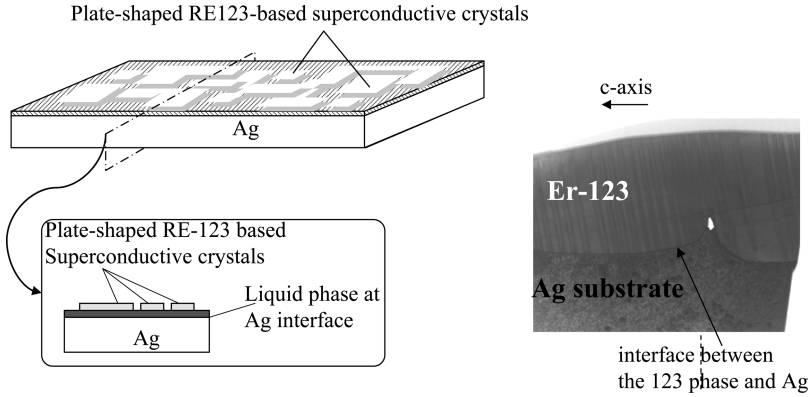

Figure 4. (left) The schematic synergistic action of Er-123 crystals production by solid phase−liquid phase reaction and the liquid phase present at the Ag substrate interface. At the melting point of Ag or lower temperature, the Er-123 crystals produced on the commercial Ag substrate were of plate shape and uniformly oriented. (right) Clean highly oriented Er-123 film on silver substrate as detected by TEM.

relatively flat and dense surface morphology. On the other hand, very large plate-like grains can be seen on the high-magnification images (Figure 2c,d). These results proved that good quality thick Er-123 films could be prepared using the solid phase−liquid phase reaction. These results were later successfully repeated with polycrystalline Ag substrates.

To determine the exact temperature for processing the films on silver substrates, a 100 nm sized powder mixture of Er-210, $BaCuO_2$, and CuO was studied by DTA in Ar-1% pO_2 atmosphere. The results are presented in Figure 1d. Two endothermic peaks on the DTA curve appeared at 840 °C (P_1) and 930 °C (P_2). It proved that the whole temperature range (P_1, P_2) can lie well below the melting point of Ag and Er_2BaO_4 can react with $Ba_xCu_yO_z$ according to reaction (2). The resulting film was composed of plate-like RE-123 single crystals uniformly oriented, with reasonably good superconducting characteristics. This experiment not only confirmed the possibility of preparing thick Er-123 superconducting films by the solid phase−liquid phase reaction on Ag substrate without the need for a buffer layer but also indicated the potential of this method for fabricating silver sheathed tapes.

Superconducting characteristics of the Er-123 thick films were found to be better when a two-step annealing process, tuned on the basis of quench experiments, was employed. The covered silver substrates were heated to 925 °C within 3 h, held there for 10 min, then cooled to 875 °C within 30 min, held at this temperature for 2 h, and finally slowly cooled to room temperature within 18 h. Superconductivity of the films was checked by means of ac susceptibility measured as a function of temperature. Figure 3a shows a sharp superconducting transition onset at 92 K, with a transition width less than 1.5 K. The films possessed *c*-axis orientation perpendicular to the substrate as indicated by the X-ray diffraction pattern of the Er-rich Er-123 sample in Figure 3b, showing a dominant (0,0,l) reflection. The surface morphology of the films observed by scanning electron microscopy is presented in Figure 3c. Large flat grains are characteristic for the film (figure left). Thickness of the Er-123 layer measured by SEM was about 10 μm. The TEM micrographs indicated a clean and clear interface between the Er-123 phase and the substrate. Scanning Hall probe measurements detected a homogeneous screening current distribution over the whole measured film surface (Figure 3d). Magnetic hysteresis loops measured by SQUID are presented in Figure 3e. The irreversibility line at 77 K along *c*-axis was about 3 T and the remanent J_c was 40 kA/cm^2 (Figure 3f). Note that the J_c-B performance can be significantly improved by lowering temperature below 77 K. We also found another way to improve the electromagnetic performance of the film, namely, by adding a small quantity of Gd-123 or Eu-123 to the Er-123 system (Figure 3g). The explanation is the following: Similarly as Y, Erbium belongs to "heavy" rare earths, atoms of which cannot sit onto Ba sites in the perovskite structure. Sizes of lighter rare earths, LRE = Gd, Eu, Sm, etc., are much closer to Ba; therefore, they occupy Ba sites and vice versa, this exchange being always present in melt-grown and other LRE-123 compounds. Because of this site occupation exchange, irregular crystallographic sites on atomic scale are formed, with dimensions close to the vortex core size, 2ξ. In this way, the LRE-123 compounds form a specific type of pinning disorder, resulting in a much better vortex pinning performance than in heavy-ion RE-123 ones.[14] Therefore, we attempted to improve vortex pinning (and the associated J_c) of the $Er_{1.2-x}Ba_2Cu_3O_y$ thin films by doping the formula by a small quantity of Gd-123. The attempt led to a significant increase of irreversibility field (Figure 3g).

The most attractive feature of the present approach is that large flat *c*-axis oriented grains grow directly on a polycrystalline Ag substrate, without any buffer layer. According to Figure 4, the interface between polycrystalline Ag substrate and the superconductor is clean and sharp, without any sign of Ag diffusion into the superconductor. Although we do not know the exact evolution of the film growth at initial stages, we speculate that the liquid phase forms a temporary insulating layer on which the flat Er-123 grains start to grow from a small number of nuclei. As the growth rate within the $a-b$ plane is higher than along *c*-axis, the growth prefers the orientation with *c*-axis perpendicular to the substrate surface (Figure 4 right). This conclusion is in accord with the study of *a*-axis SmBaCuO films growth on single crystalline substrates.[15] Later, the liquid phase interlayer builds up into the film structure and disappears.

Note that RE_2BaO_4 is stable at temperatures around melting of the intermediate (liquid) phase. However, RE-123 and especially RE-211 are even more stable, the former being decomposed into the latter according to reaction 1 at temperatures higher than P_2 (> P_1). Thus, RE-211 releases from RE-123 only at a temperature higher than P_2, much higher than the melting point of the liquid phase in our process. The stability of RE-123 and RE-211 does not allow for another composition of the liquid phase in reaction 1 but $Ba_2Cu_5O_x$. In contrast, from the scheme of reaction 2 one can deduce the liquid phase composition as $BaCu_2O_x$ with $x \approx 3$, if all BaCuO and CuO react. The difference in composition is probably the reason for

different melting temperatures of the liquid phases (the $Ba_2Cu_5O_x$ is also frequently used as a solvent in the regular liquid phase epitaxy). The combination chosen in our work seems to be optimal.

Another aspect, interesting mainly from an industrial point of view, is that for drawing of a metal-sheathed superconductor into wires or tapes, the sheath material has to satisfy two important conditions, namely, (i) be chemically inert to the liquid phase formed in the solid phase−liquid phase reaction and (ii) allow permeation of oxygen during the additive annealing in. Ag used in our approach excellently satisfies both these conditions.

4. Conclusion

In summary, a new process was found enabling for the first time formation of uniformly oriented RE-123 crystals on a silver polycrystalline substrate without the need for a buffer layer or application of external pressure for orienting the crystals. The present results show that the new solid phase−liquid phase reaction is promising for fabrication of thick Er-123 superconducting films not accessible by conventional methods. Such a process can be easily adapted for fabrication of long tapes or wires, especially using the powder-in-tube (PIT) technology developed for BiSCCO tapes. Consequently, the present invention can be widely utilized for construction of apparatuses generating strong magnetic fields, for high currents transmission, and energy saving setups.

Acknowledgment. This work was supported by the New Energy and Industrial Technology Development Organization (NEDO). One of the authors, M.J., acknowledges support of the GACR Grant No. 202/08/0722 and the Research Aim AVOZ 10100520.

References

(1) Bednorz, G.; Muller, K. A. *Z. Phys. B* **1986**, *64*, 189.
(2) Wu, M. K.; Ashbum, J. R.; Torng, C. J.; Hor, P. H.; Meng, R. L.; Gao, L.; Huang, Z. J.; Wang, Y. Q.; Chu, C. W. *Phys. Rev. Lett.* **1987**, *58*, 908.
(3) Heine, K.; Tenbrink, J.; Thoner, M. *Appl. Phys. Lett.* **1989**, *55*, 2441.
(4) Robert, F. S. *Science* **2005**, *308*, 348.
(5) Robert, F. S. *Science* **2002**, *295*, 786.
(6) Okazaki, T.; Hyashi, K.; Sato, K. *SEI Techn. Rev.* **2006**, *61*, 24.
(7) Kohno, O.; Ikeno, Y.; Sadakata, N.; Goto, K. *Jpn. J. Appl. Phys.* **1988**, *27*, L77.
(8) Larbalestier, D.; Gurevich, A.; Matthew, F.; Anatoly, P. D. *Nature* **2001**, *414*, 368.
(9) Foltyn, S. R.; Civale, L.; MacManus-Driscoll, J. L.; Jia, Q. X.; Maiorov, B.; Wang, H.; Maley, M. *Nat. Mater.* **2007**, *6*, 631.
(10) Ghalsasi, S.; Zhou, Y. X.; Chen, J.; Lv, B.; Salama, K. *Supercond. Sci. Technol.* **2008**, *21*, 045015.
(11) Hirata, H.; Sakai, N.; Hirabayashi, I.; Murakami, M.; Tanaka, S. *J. Jpn. Soc. Microgravity Appl.* **2006**, *23*, 210.
(12) Muralidhar, M.; Sakai, N.; Murakami, M.; Hirabayashi, I.; Tanaka, S. *Physica C* **2006**, *445−448*, 282.
(13) Chen, D. X.; Goldfarb, P. R. *J. Appl. Phys.* **1989**, *66*, 2489.
(14) Muralidhar, M.; Sakai, N.; Chikumoto, N.; Jirsa, M.; Machi, M.; Nishiyama, M.; Wu, Y.; Murakami, M. *Phys. Rev. Lett.* **2002**, *89*, 237001.
(15) Tang, C. Y.; Cai, Y. Q.; Li, W.; Sun, L. J.; Yao, X.; Jirsa, M. *Cryst. Growth Des.* **2009**, *9*, 1339−1343.

CG8012987